J Appl Electrochem (2010) 40:621–630
DOI 10.1007/s10800-009-0037-6

ORIGINAL PAPER

Behaviour of Al–Ga alloy during cathodic polarization

A. Višekruna · J. Radošević · S. Slavica Matešić · N. Krnić

Received: 1 May 2009 / Accepted: 23 November 2009

Abstract The effect of the addition of small quantities of gallium to high-purity aluminium (99.999 wt%) on its electrochemical behaviour at high cathodic potentials (up to −2.0 V versus SCE), has been investigated using the potentiostatic pulse method. After cathodic polarization, anodic current was traced versus time to determine the quantity of charge necessary for oxidation of substances formed. Anodic current responses to the return to the E_{OCP} were also recorded in the period of 1 s. Time responses of the cathodic and anodic currents were analyzed. The cyclic voltammetry method was used to determine the hydration potential. The range of low and high cathodic potentials (LCP, HCP) was defined for all the samples. It has been established that the oxide film retains its properties in the LCP range, while in the HCP range cathodic breakdown and hydration of the oxide take place. Electrochemical methods complemented the SEM and EDAX analysis before and after the cathode pulse of −1.9 V versus SCE.

Keywords Aluminium activation · Al–Ga alloy · Cathodic polarization · Hydration potential

1 Introduction

Corrosion processes have been extensively investigated in pure aluminium [1, 2].

Aluminium alloys are widely used in everyday practice, primarily as construction materials, due to their exceptional mechanical properties and corrosion resistance. The main reason for the corrosion resistance of aluminium is the formation of a thin compact oxide film on the surface of the metal. The standard reversible potential of aluminium ($E^0_{\mathrm{Al/Al^{3+}}} = -1.66$ V versus NHE [3]) and its high energetic capacity (2,980 A h $\mathrm{kg^{-1}}$) are very attractive properties when aluminium is used as active anodic material in sacrificial anodes in cathodic protection system or in chemical power sources. However, pure aluminium is practically impossible to use, because a protective oxide film forms on it, making the potential positive, which in turn makes aluminium unattractive as energetic material.

In recent years, increasing attention has been given to a number of aluminium alloys, in which aluminium is electrochemically active, e.g. with In, Ga, Sn, Hg and Bi [4–6].

According to Reboul and associates alloying elements influent to the creation of active sites on the grain border of the base metal and extracted alloying element which allows progression of anodic process [7].

Valand and Nilsson depassivation of the aluminium attributed to embedding the alloying elements in aluminium oxide film, when change of properties of film occurred

A. Višekruna
Aluminij d.d. Mostar, Baćevići b.b., 88000 Mostar, Bosnia and Herzegovina
e-mail: antonija.visekruna@aluminij.ba

J. Radošević
Department of Electrochemistry and Materials Protection, Faculty of Chemical Technology, Teslina 10/V, 21000 Split, Croatia
e-mail: rjagoda@ktf-split.hr

S. Slavica Matešić (✉)
TLM d. d., Narodnog preporoda 12, 22000 Šibenik, Croatia
e-mail: sanja.slavica@si.t-com.hr

N. Krnić
Department of Mechanical Technology, Faculty of Electrical, Mechanical Engineering and Naval Architecture, Ruđera Boškovića b.b., 21000 Split, Croatia
e-mail: niksa.krnic@fesb.hr

and also shifting of corrosion potential to more negative values [8].

Activation of aluminium can be also achieved if small quantities of suitable metal cations, such as In^{3+}, Ga^{3+}, Hg^{2+}, Sn^{4+} or Sn^{2+}, are added to the electrolyte [9–17].

In this study, an attempt has been made to examine the behaviour of Al–Ga alloys during cathodic polarization up to high negative potential values.

2 Experimental

The Al–Ga binary alloys obtained by courtesy of Alcan International Ltd. had been prepared with different contents of gallium as the alloying component (0.01, 0.02, 0.05, 0.1, 0.2 and 2.6 wt%) in high-purity (99.999 wt%) aluminium. The Al–Ga alloys were cut into cubes of 1 cm^3, which were made into electrodes by inserting an electrical contact wire into one of the sides and insulating that and other four sides by an epoxy resin, so that only one face was open to the electrolyte. Before each experiment, the open side was mechanically polished to a mirror finish, degreased in alcohol and left in the air to acquire the “natural” oxide film, prior to immersion into the solution.

The standard closed electrochemical cell was used with a saturated calomel electrode (SCE) as the reference electrode and platinum counter electrode in separate compartments. The solution was 2 M NaCl, which was purged free of oxygen by purified nitrogen. The temperature was maintained at 25 ± 0.1 °C. Electrochemical measurements were performed with a computer driven potentiostat (PAR M273A).

Potential sweeps at a very low sweep rate (0.5 mV s^{-1}) were applied to the Al–Ga electrodes starting from the pitting potential in the negative direction down to −2.0 V versus SCE and back. The current response was converted to a logarithmic scale and the resulting Tafel plots.

The potentiostatic pulse method was also used to record the time dependence of the cathodic current density on the electrode potential pulses ranging from −1,150 to −2,000 mV versus SCE with pulse duration of 1 s, which appears after a certain cathodic polarization, when the potential returns to a value slightly more positive than the open circuit potential (OCP).

Samples of Al–Ga alloys were observed by a scanning electron microscope (SEM) applying the scanning method prior to and after the cathodic pulse of −1,900 mV and duration of 1 s. The elemental composition of the surface of the same samples was observed by EDAX analysis (OXFORD EDS Energy Dispersive Analysis System).

3 Results and discussion

3.1 Open circuit potential (E_{OCP})

The time dependence of the open circuit potential (E_{OCP}) on the content of Ga 0.2 and 2.6 wt% in the alloy at a pH 6 was examined over a period of 36 h and was shown in Fig. 1. The OCP of super pure aluminium in a 2-M NaCl solution varied approximately 40 mV about the value of −1,120 mV versus SCE [1]. The time needed to reach a stable E_{OCP} value was 10 h in this case.

With the alloy containing 0.2 wt% Ga, the E_{OCP} shifts slightly to the negative direction (~70 mV) relative to pure Al, while this value increases as high as 300 mV relative to pure Al in the case of the alloy with a higher Ga content (2.6 wt%).

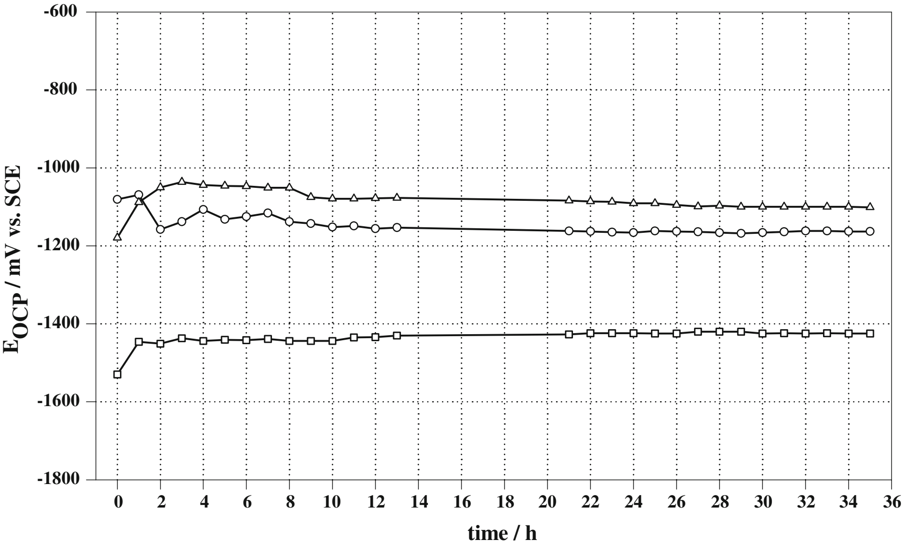

Fig. 1 Open circuit potential (E_{OCP}) versus time for (*open triangle*) 5 N Al, (*open circle*) 5 N Al–0.2 wt% Ga, (*open square*) 5 N Al–2.6 wt% Ga in 2 M NaCl at a pH value of 6

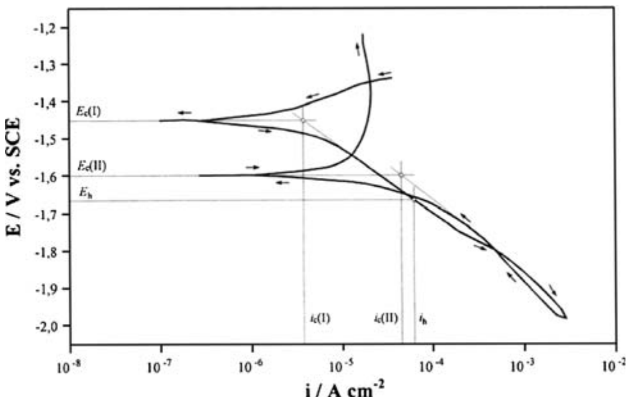

Fig. 2 Tafel plots for 5 N Al–0.02 wt% Ga in a 2 M NaCl solution (pH = 7)

3.2 Polarization measurements

During cathodic polarization of Al–Ga alloys with small Ga contents (0.01, 0.02 and 0.05 wt%), no significant change with respect to the Tafel plot for pure aluminium has been noted [18].

Figure 2 shows a typical plot obtained in 2 M NaCl with pH 7 for the 0.02 wt% Ga alloy. When the potential changes in the negative direction, a corrosion potential E_c(I) appears, followed by a region of a high increase in current. At the potential of approximately −1,660 mV versus SCE, designated as the hydration potential, E_h, the current response deviates from the linear Tafel line and leads to orders of magnitude larger current densities. The significant changes found at the potentials beyond E_h reflect oxide hydration and penetration at the interface, at which hydrogen evolution takes place all the way to the metal surface.

The chemical attack by OH^- ions and water seems to be dominant in the dissolution of the metal [19]. The current model of cathodic behaviour of aluminium [20] assumes that the hydration of the oxide film takes place as a consequence of increased alkalinity at the oxide/solution interface. Kunce [21] and Diggle [22] have found that at a certain critical negative potential, a sudden rise occurs not only in the hydrogen evolution rate, but also in that of metal dissolution. When the potential returns in the positive direction, the current response diverges and a new corrosion potential appears, E_c(II), which is much more negative than E_c(I).

Table 1 shows the parameters obtained from voltammograms for different pH values, with parameters of the

Table 1 Characteristic features of the cathodic Tafel plots for aluminium and 5 N Al–Ga alloys in a 2 M NaCl solution

pH	E_c(I) (mV)	i_c(I) (μA cm^{-2})	E_c(II) (mV)	i_c(II) (μA cm^{-2})	E_h (mV)	i_h (μA cm^{-2})
Al(5 N) [18]						
5	−1,170	4.00			−1,480	10.00
Al–0.01% Ga						
1	−1,000	19.00	−965	16.00	−1,485	60.00
2	−1,295	0.47	−1,470	2.80	−1,620	34.00
3	−1,310	1.65	−1,460	0.90	−1,590	38.00
4	−1,285	0.84	−1,420	1.00	−1,600	30.00
5	−1,320	0.76	−1,465	1.00	−1,580	16.00
6	−1,360	0.69	−1,510	1.00	−1,620	21.00
7	−1,370	2.40	−1,575	0.84	−1,630	24.00
8	−1,395	0.56	−1,470	0.90	−1,685	58.00
9	−1,700	40.00	−1,625	220.00	−1,915	1,400.00
10	−1,968	185.00	−1,850	220.00	−1,970	1,250.00
Al–0.02% Ga						
1	−1,200	13.00	−1,050	7.00	−1,630	160.00
2	−1,405	3.50	−1,620	39.00	−1,670	115.00
3	−1,370	5.40	−1,605	40.00	−1,715	165.00
4	−1,435	3.10	−1,620	32.00	−1,725	145.00
5	−1,380	3.60	−1,600	72.00	−1,695	98.00
6	−1,400	2.60	−1,600	5.20	−1,680	60.00
7	−1,452	3.80	−1,600	48.00	−1,660	64.00
8	−1,410	2.70	−1,585	19.50	−1,670	71.00
9	−1,655	98.00	−1,635	440.00	−1,900	2,950.00
10	−1,830	450.00	−1,830	295.00	−1,965	1,800.00

Table 1 continued

pH	E_c(I) (mV)	i_c(I) (μA cm^{-2})	E_c(II) (mV)	i_c(II) (μA cm^{-2})	E_h (mV)	i_h (μA cm^{-2})
Al–0.05% Ga						
1	−980	54.00	−1,090	6.60	−1,335	400.00
2	−1,150	9.80	−1,050	0.90	−1,440	110.00
3	−1,170	2.90	−1,495	2.90	−1,430	8.00
4	−1,230	1.70	−1,550	7.00	−1,475	14.00
5	−1,290	0.51	−1,505	5.10	−1,560	24.00
6	−1,260	0.72	−1,375	2.50	−1,440	8.10
7	−1,270	0.65	−1,540	7.90	−1,730	230.00
8	−1,295	0.46	−1,480	3.00	−1,755	290.00
9	−1,150	0.90	−1,465	3.00	−1,550	69.00
10	−1,452	5.10	−1,449	2.10	−1,610	42.00
Al–0.1% Ga						
1	−950	320.00	−970	54.00	−1,480	1,900.00
2	−1,130	14.00	−1,105	2.50	−1,435	190.00
3	−1,220	8.00	−1,175	5.40	−1,600	190.00
4	−1,250	8.90	−1,310	0.65	−1,500	14.00
5	−1,260	1.70	−1,360	1.90	−1,525	14.00
6	−1,290	1.50	−1,340	0.79	−1,500	14.00
7	−1,310	1.00	−1,310	3.00	−1,650	79.00
8	−1,320	3.10	−1,345	1.40	−1,695	125.00
9	−1,375	4.10	−1,275	1.40	−1,690	90.00
10	−1,480	2.60	−1,310	2.10	−1,650	61.00
Al–0.2% Ga						
1	−930	270.00	−901	180.00	−1,380	1,250.00
2	−1,125	7.00	−1,040	1.60	−1,400	100.00
3	−1,100	9.00	−1,100	5.00	−1,475	55.00
4	−1,190	4.10	−1,190	3.00	−1,460	22.00
5	−1,250	1.20	−1,225	2.00	−1,450	8.40
6	−1,250	0.80	−1,240	4.90	−1,445	8.40
7	−1,280	0.92	−1,266	2.60	−1,500	20.00
8	−1,300	0.65	−1,320	3.80	−1,675	170.00
9	−1,400	2.80	−1,370	2.40	−1,615	80.00
10	−1,500	9.00	−1,420	12.00	−1,625	80.00
Al–2.6% Ga						
1	−1,475	3,100.00	−1,475	760.00	−1,935	7,000.00
2	−1,470	230.00	−1,470	145.00	−1,840	3,400.00
3	−1,495	55.00	−1,385	3.90	−1,840	1,900.00
4	−1,490	59.00	−1,375	1.90	−1,840	2,000.00
5	−1,490	38.00	−1,375	1.30	−1,845	1,600.00
6	−1,560	50.00	−1,655	29.00	−1,850	2,100.00
7	−1,565	65.00	−1,660	28.00	−1,870	2,100.00
8	−1,700	60.00	−1,780	70.00	−1,840	690.00
9	−1,735	75.00	−1,830	95.00	−1,850	850.00
10	−1,700	250.00	−1,865	390.00	−1,850	880.00

cathodic Tafel functions characterizing the cathodic process, such as corrosion potentials E_c(I) and E_c(II) and corrosion currents i_c(I) and i_c(II) for the negative and the positive direction sweep responses, as well as the points of occurrence of hydration of the oxide layer characterized by E_h and i_h.

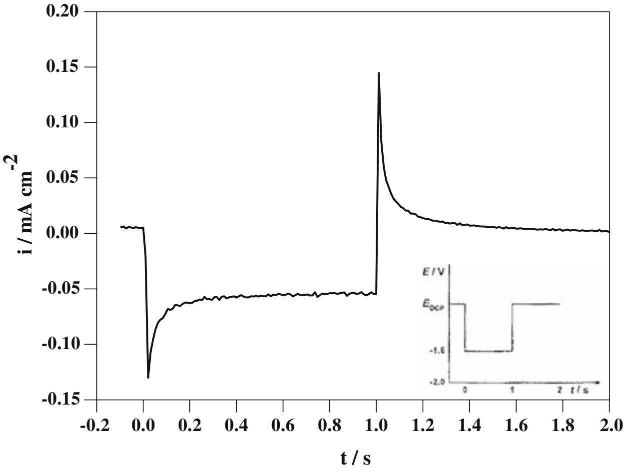

Fig. 3 Sequences of cathodic and anodic current–time responses to the potential pulse from −1,600 mV versus SCE and back for 5 N Al–0.02 wt% Ga; pulse duration: 1 s

Figure 3 shows a typical current–time response during the cathodic polarization of the 5 N Al–0.02 wt% Ga alloy, obtained with a potentiostatic pulse registered in the 2 M NaCl solution.

Figure 4 shows the characteristic series of current responses for the series of cathodic pulses increasing by 50 mV (in the range from −1,200 to −2,000 mV) with the duration of 1 s at each cathodic potential.

Two potential domains have been found. At lower cathodic potentials (to −1,700 mV), the pulsation results in typical potentiostatic charging curves in which the current shows the characteristic exponential decay, while at higher cathodic potentials the dependence of current on time is much more complex.

The area under the cathodic current–time response represents the quantity of charge spent on reduction, Q_c [1], and the values obtained for each alloy within 1 s. Table 2 presents the values obtained.

The values of Q_c increase with the increase of the gallium content in the alloy and also with the cathodic potential values. They differ greatly in two regions of the cathodic potential: LCP (low cathodic potential), for alloys containing smaller amounts of gallium, and HCP (high cathodic potential). The exception is Al–2.6 wt% Ga alloy. On the alloy with 2.6% Ga, it can be seen the smaller value of Q_c in relation to the alloy with lower content of Ga, which could be explained by the fact that the beginning of hydration of oxide film in that alloy has been shifted towards negative potential values as a result of which during the cathode process the creation of the substances on the metal surface has been significantly reduced.

From the results obtained, it is possible to define for all the alloys the potential range in which the cathodic breakdown occurs and the oxide film hydrates.

The more negative the potential, the more intense the release of hydrogen from water, leaving behind the equivalent quantity of OH^- ions that attack the oxide surface, with the final result of hydration of the oxide layer. The hydration layer represents a resistance to ion transfer into the solution [23]. Hunter et al. [24] have established that when the potential is shifted in the negative direction on the surface of Al–Ga alloys superactivity occurs. Superactivity is caused only by the presence of the solid state Ga. In the region of HCP, in the alkaline medium, a relatively high concentration of OH^- ions has been created. During cathodic polarization, the (species) ion $[HGaO_3]^{2-}$ could be created [25].

By integrating current with time [1] at the return of the potential to the rest value, quantities of charge, Q_A, have been evaluated for each alloy for 1 s as shown in Table 3. It is obvious that, with the increase in the gallium content in the alloy, the Q_A value increases too. The exception is Al–2.6 wt% Ga alloy in which the amount at the substance which oxidizes has been much smaller compared to the previously mentioned alloys.

Breslin and Carrol [25] consider that the removal of the oxide film by cathodic polarization results in hydrogen extraction. When hydrogen extraction starts on those small local surfaces, the value of pH increases due to the growing volume of hydrogen bubbles. pH values inside the micropits, created between bubbles and the electrode surface, has higher pH values than that of the electrolyte. This condition helps in creation of hydrated forms such as $[GaO_2]^-$, $[HGaO_3]^{2-}$ and $[GaO_3]^{3-}$. The extraction of hydrogen is probably followed by the deposition of Ga. This fast creation of hydrogen pockets has a consequence of the breakdown of the oxide film, nucleation and increasing of cracks.

Shirkhanzadeh et al. [26] assumed that $[HGaO_3]^{2-}$ have been reduced according to the following reaction (1):

$$[HGaO_3]^{2-} + 5\ H^+ + 3\ e^- \rightarrow Ga + 3\ H_2O. \quad (1)$$

The combined effect of gallium-enriched surface, presence of gallium as a solid solution, and its accumulation on granular inter-boundary surfaces contributes to activation.

Because of its low melting point [24], gallium first stays on the electrode surface as a highly mobile atom or atom groups. These mobile groups then accumulate on inter-boundary metal/solution surfaces. Superactivity occurs as a consequence of the local “wrapper unwinding” process which occurs due to the retention and agglomeration of highly mobile Ga atoms on the surface. This explains the difference in the Ga content in individual places, which has been found by EDAX analysis.

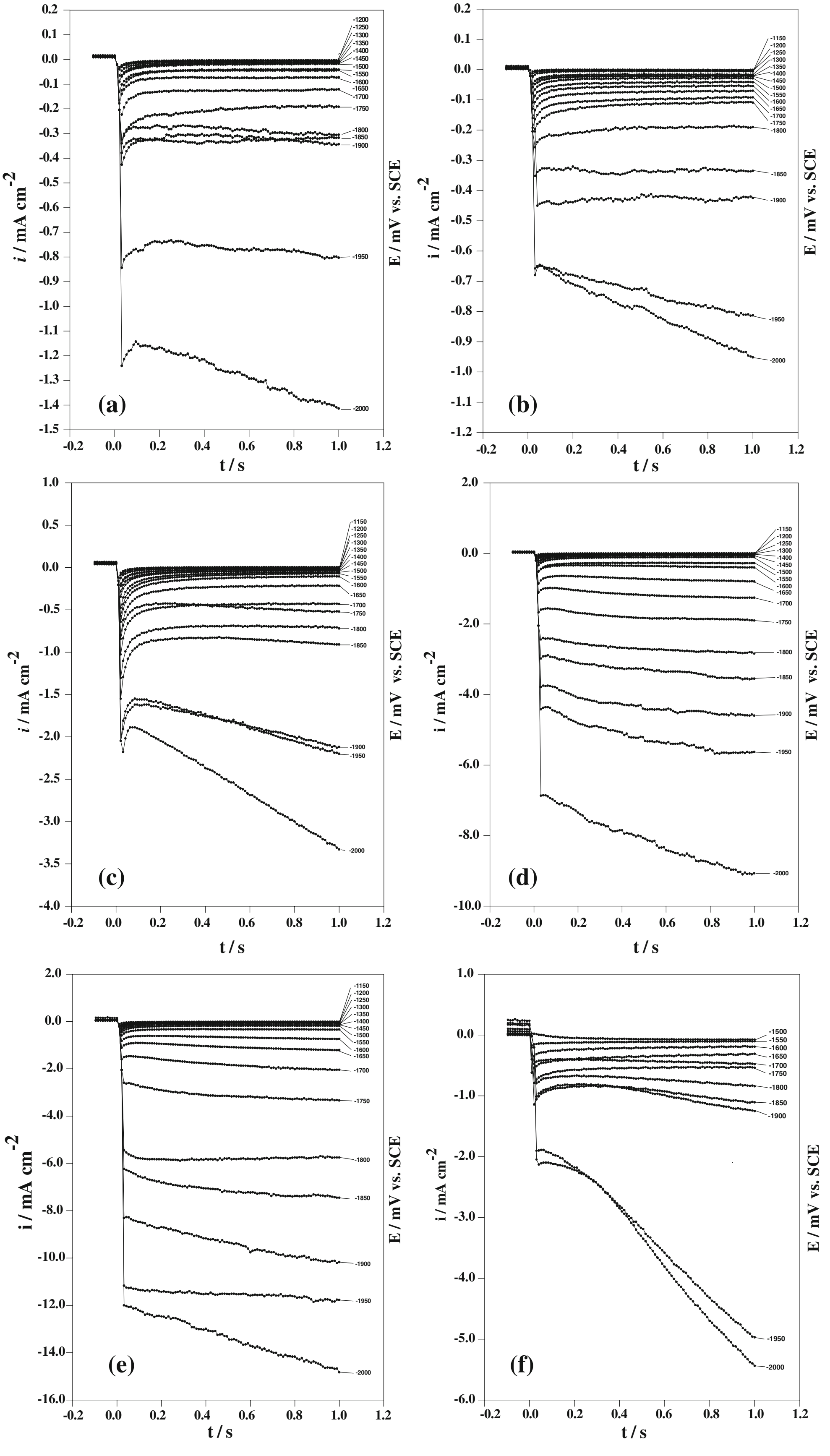

Fig. 4 Sequences of cathodic current–time responses to the potential pulse from E_{OCP} to different negative values in 2 M NaCl for **a** 5 N Al–0.01 wt% Ga, **b** 5 N Al–0.02 wt% Ga, **c** 5 N Al–0.05 wt% Ga, **d** 5 N Al–0.1 wt% Ga, **e** 5 N Al–0.2 wt% Ga and **f** 5 N Al–2.6 wt% Ga; pulse duration: 1 s

Table 2 The values for the quantity of charge Q_c, obtained for Al–Ga alloys at different cathodic potentials at cathodic pulse duration of 1 s

	E / mV	Q_c / μC cm^{-2}					
		0.01% Ga	0.02% Ga	0.05% Ga	0.1% Ga	0.2% Ga	2.6% Ga
LCP	-1,050						
	-1,100						
	-1,150		0.75	2.01	3.75	13.23	
	-1,200	2.42	3.38	9.21	11.46	26.45	
	-1,250	4.36	5.38	17.64	24.39	35.71	
	-1,300	7.07	18.76	41.41	38.33	53.85	
	-1,350	12.36	18.03	36.88	40.65	63.51	
	-1,400	17.10	23.67	62.68	65.70	79.30	
	-1,450	20.90	23.32	68.88	96.82	130.20	
	-1,500	22.53	31.43	104.10	150.00	195.50	45.00
	-1,550	46.62	45.95	131.40	337.20	338.30	106.30
	-1,600	47.42	58.82	177.60	449.70	662.60	197.10
	-1,650	76.06	77.25	262.20	886.60	1,054.00	349.00
	-1,700	128.00	101.50	301.30	1,421.00	1,777.00	425.70
HCP	-1,750	205.70	219.70	545.20	2,194.00	3,037.00	542.20
	-1,800	279.80	295.70	850.50	3,285.00	5,644.00	720.40
	-1,850	316.50	328.40	1,032.00	4,026.00	6,919.00	926.90
	-1,900	320.40	415.60	2,158.00	5,272.00	9,125.00	954.60
	-1,950	749.80	718.10	2,161.00	6,341.00	11,250.00	3,203.00
	-2,000	1,238.00	782.10	2,984.00	9,893.00	13,050.00	3,390.00

Table 3 The values for charge Q_A for Al–Ga alloys, determined after termination of cathodic polarization lasting 1 s and after return of the potential to the rest value

E (mV)	Q_A (μC cm^{-2})					
	0.01% Ga	0.02% Ga	0.05% Ga	0.1% Ga	0.2% Ga	2.6% Ga
−1,050						
−1,100						
−1,150		2.79	23.39	26.65	33.10	
−1,200	13.83	15.01	24.07	53.53	55.20	
−1,250	15.06	19.73	37.21	54.93	54.48	
−1,300	15.34	22.55	33.76	40.99	47.15	
−1,350	17.74	22.93	38.82	53.93	61.15	
−1,400	17.16	23.71	60.86	70.39	71.07	
−1,450	18.36	27.25	62.70	70.20	70.78	
−1,500	19.04	25.74	65.70	71.32	78.86	23.49
−1,550	24.57	26.54	85.00	86.76	89.43	34.28
−1,600	20.24	31.26	116.50	127.80	139.50	35.44
−1,650	24.22	33.79	147.90	213.60	232.90	40.73
−1,700	34.58	35.31	147.10	215.30	364.00	41.77
−1,750	43.21	51.04	174.50	252.30	657.30	40.26
−1,800	48.66	52.26	193.60	285.00	1,033.00	47.34
−1,850	41.26	64.99	237.20	324.50	1,452.00	48.36
−1,900	62.15	81.39	305.00	371.50	2,764.00	51.81
−1,950	94.77	169.44	329.60	412.10	2,195.00	53.48
−2,000	176.40	200.90	467.90	672.80	3,180.00	96.95

Fig. 5 SEM micrographs and the EDAX analysis of a polished sample of the 5 N Al–0.2 wt% Ga alloy, enlarged ×600

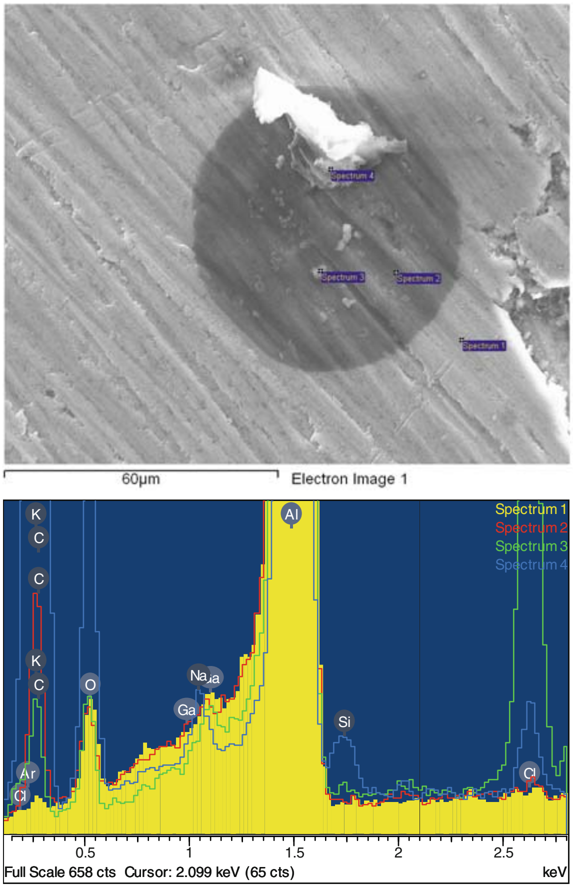

Elements %	C	O	Na	Al	Si	Cl	Ar	K	Ga	Total
Spectrum 1		3.88		95.64		0.09	0.13		0.26	100.00
Spectrum 2	26.44	3.16		70.09		0.16	0.06		0.10	100.00
Spectrum 3	20.52	5.33		63.07		5.73	-0.02	4.71	0.65	100.00
Spectrum 4	74.52	9.02	0.21	15.62	0.13	0.29	-0.01	0.19	0.02	100.00

3.3 Examination of the surface morphology and composition

A scanning electron microscope was used to examine the previously polished surface with 0.2 wt% Ga content, Fig. 5. It has been found that Ga occurs in isolated phases on this alloy. This behaviour of Ga explains why the Ga content is considerably different at locations 1, 2 and 3, while both Ga and Al have been covered by high carbon content at point 4 on the electrode surface.

Figure 6 shows that surface change occurred at some places for the sample of the same alloy after a −1,900 mV cathodic pulse during 1 s. The moveable groups of Ga atoms accumulated on the metal/solution interface causing the aluminium pitting corrosion.

After cathodic pulse, the sample underwent changes at some places on the surface. The EDAX analysis has shown the differences in Ga contents at certain points. The Ga content is very high (0.53%) at point 1, while Ga has not been found at all points 3 and 4, because in those potential areas, the $[HGaO_3]^{2-}$ species can be formed, with Ga leaving the aluminium surface in that way (in those places). The EDAX analysis has also shown that at these places where the Ga content is high, the content of Cl is very high, probably because the Ga on the electrode surface stimulates Cl adsorption and so encourages the activation effect [27].

4 Conclusion

When small quantities of Ga are added to high-purity aluminium in a 2 M NaCl solution, changes in its behaviour during cathodic polarization occur.

Based on the results obtained, the potential range in which the cathodic breakdown of the oxide film occurs has been defined for all the samples.

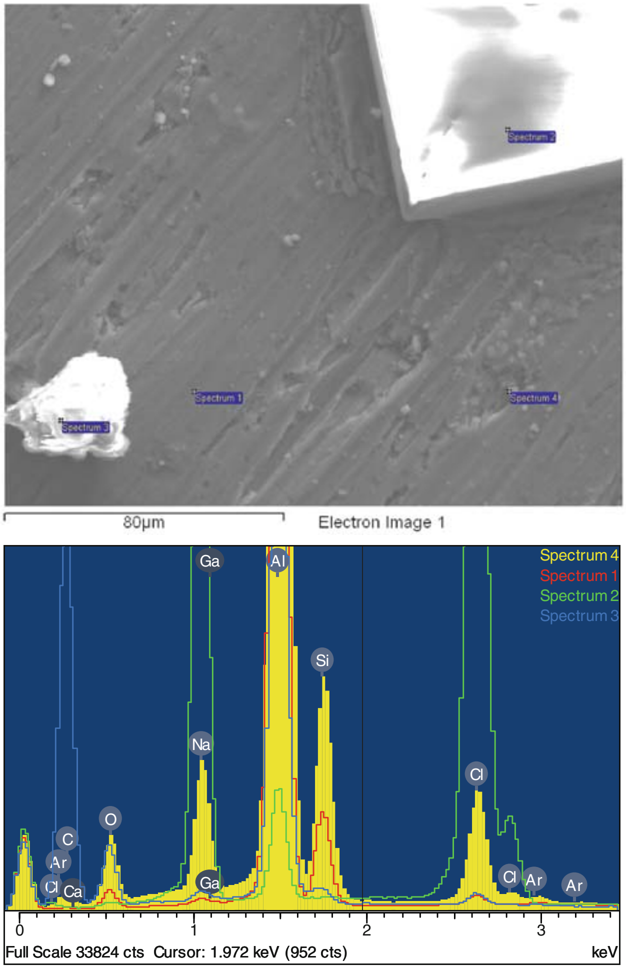

Fig. 6 SEM micrographs and the EDAX analysis of a polished sample of the 5 N Al–0.2 wt% Ga alloy after a cathodic pulse (−1,900 mV); pulse duration: 1 s, enlarged ×800

Elements %	C	O	Na	Al	Si	Cl	Ca	Ga	Total
Spectrum 1	2.25	8.98	0.43	70.66	15.68	1.47		0.53	100.00
Spectrum 2		1.37	35.02	6.16	0.06	57.19	0.15	0.06	100.00
Spectrum 3	69.77	14.38	0.32	14.82	0.31	0.40			100.00
Spectrum 4	15.01	12.36	4.23	52.02	10.96	5.42			100.00

In the range of lower cathodic potentials (LCP), the oxide film retains its properties, while in the range of higher cathodic potentials (HCP) cathodic breakdown and hydration of the oxide layer take place. The boundary between these two potential ranges shifts towards more negative potential values when the Ga content in the alloy increases. The exception is Al–2.6 wt% Ga alloy.

Cyclic voltammetry has shown that at all pH values (except at pH 1 and 2, where cathodic processes include the H^+ ion reduction), the presence of Ga affects the anodic process as well as the corrosion potential. The cathodic process takes place throughout the oxide film by reduction of water molecules.

References

1. Radošević J, Kliškić M, Dabić P, Stevanović R, Despić A (1990) J Electroanal Chem 277:105
2. Despić A, Radošević J, Dabić P, Kliškić M (1990) Electrochim Acta 35:1743
3. Pourbaix M (1974) Atlas of electrochemical equilibria in aqueous solutions. NACE, Houston, TX
4. Reading JT, Newport JJ (1966) Mater Protect 5:15
5. Mance A, Cerović D, Mihajlović A (1984) J Appl Electrochem 14:459
6. Keir DS, Prior MJ, Sperry PR (1969) J Electrochem Soc 116:319
7. Reboul MC, Gimenez Ph, Rameau JJ (1983) Corrosion 83:214
8. Valand T, Nilsson G (1977) Corros Sci 17:931
9. Carroll WM, Breslin CB (1992) Corros Sci 33:1161
10. Breslin CB, Carroll WM (1993) Corros Sci 34:327
11. Saidman SB, Bessone JB (1997) J Appl Electrochem 27:731

12. Saidman SB, Bessone JB (1997) Electrochim Acta 42:413
13. Venugopal A, Veluchamy P, Selvam P, Minoura H, Raja VS (1997) Corrosion 53:808
14. Venugopal A, Raja VS (1997) Corros Sci 39: 1285; 2053
15. El Shayeb HA, Abd El Wahab FM, Zein El Abedin S (1999) J Appl Electrochem 29:479
16. Breslin CB, Rudd AL (2000) Corros Sci 42:1023
17. Bessone JB (2006) Corros Sci 48:4243
18. Radošević J, Kliškić M, Despić A (1992) J Appl Electrochem 22:649
19. Keasche H (1963) Werkst Corros 14:557
20. Nisancioglu K, Holtan H (1979) Electrochim Acta 24:1229
21. Kunce J (1967) Corros Sci 7:273
22. Diggle JW, Downie TC, Goulding CW (1968) Corros Sci 8:907
23. Van De Ven EPGT, Koelmans H (1976) J Electrochem Soc 123:143
24. Hunter JA, Scamans GM, Sykes J (1993) Int Power Symp 17:193
25. Breslin CB, Carroll WM (1992) Corros Sci 33:1735
26. Shirkhanzadeh M, Thompson GE (1988) Electrochim Acta 33:939
27. El Shayeb HA, Abd El Wahab FM, Zein El Abedin S (2001) Corros Sci 43:643